CHAPTER 9

The Functional Relationship of the column Calibration Factor in Thermal Diffusion Column Measurement

The functional relationship of the column calibration factor in thermal diffusion column measurement

9.1. Introduction

The thermal diffusion column (TDC) is a very useful device for concentrating impurities of a gas. The enrichment of impurities becomes squared when the length of the column is doubled. The TDC is also used to determine the thermal diffusion factor α_T of any isotopic or nonisotopic gas mixture. The column theory, on the other hand, may be improved by the accurate experimental determination of α_T of the binary gas mixture in a column. Again, the close correlation of α_T with the molecular force parameters allows one to locate the exact force parameters of the interacting molecules. Thus both from experimental and from theoretical points of view, an accurate estimation of α_T is necessary.

In the absnce of a theoretical possibility of estimating the actual experimental α_T from the existing column theory, Acharyya *et. al* [1] and Datta *et. al* [2], however, introduced a scaling factor F_s called the column calibration factor (CCF) into the relation :

$$\ln q_{max} = \alpha_T F_s (r_c, r_h, L, \bar{T}) \qquad \text{..... (9.1)}$$

r_c and r_h are the cold and hot wall radii of a given column of geometrical length L and $\bar{T} = (T_h + T_c)/2$, T_h and T_c being the hot and cold wall temperatures in kelvin respectively. Here $\ln q_{max}$ is the maximum value of $\ln q_e$ at the optimum pressure and q_e is the equilibrium separation factor. Although, the model independency of F_s is well established[3] for its important role in the estimation of reliable α_T[1-4], the functional relationship of F_s with r_c, r_h, L and $\bar{T}$ remains unknown.

Rutherford and Kaminsky[5] had measured the column coefficients H', K'_c and K'_d using Ne^{20}-Ne^{22} gas mixtures with their natural isotopic abundances at various experimental temperatures in four different columns; see Table 9.1. The hot Nichrome V wire of their[5] I, II and III TD columns had radius r_h = 8×10^{-4}m. Their column IV was a thin-walled Nichrome V tube of radius r_h=3.2x

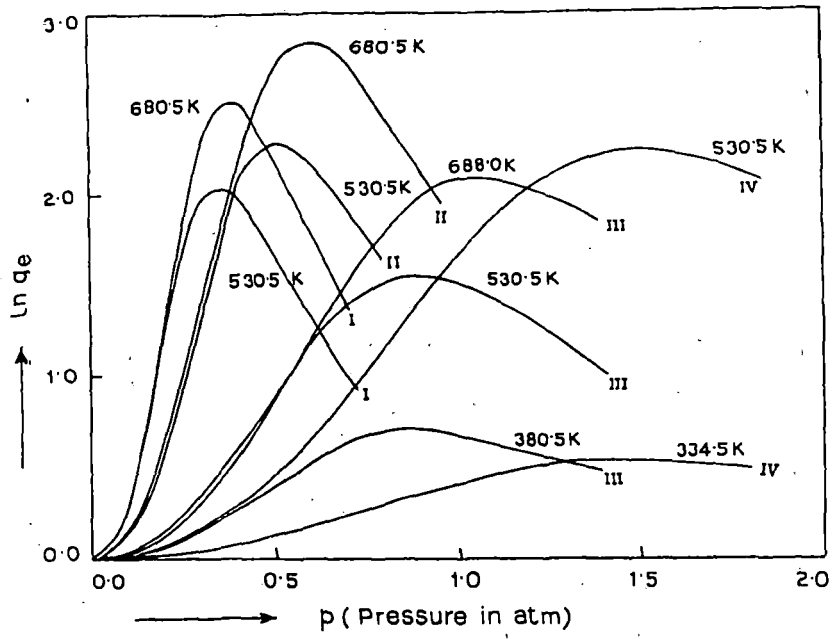

Fig. 9.1. A plot of the $\ln q_e$ against the pressure p in atmospheres of Ne^{20}–Ne^{22} mixtures : curve I, for column I at 530.5 K and 680.5K; curve II, for column II at 530.5 K and 680.5K; curve III, for column III at 380.5 K, 530.5 K and 688.5 K; and curve IV, for column IV at 334.5 K and 530.5 K.

10^{-3}m. The radii of water-cooled metal tubes of all these columns were r_c=1.6 x 10^{-2} m, 1.27 x 10^{-2} m, 9.43 x 10^{-3} m and 9.43 x 10^{-3} m respectively. The geometrical length of columns I and II was L = 3.05 m whereas columns III and IV had L=1.534 m. This inspired us to observe α_T values from the pressure dependences of $\ln q_e$ values of Ne^{20}- Ne^{22} mixtures at the experimental temperatures. The $\ln q_e$ of Ne^{20}-Ne^{22} gas mixtures as a function of the atmospheric pressure are shown in Fig. 9.1 by the least square fitted curves for these columns. The H', K'_c and K'_d[5] are used to study the temperature dependence of α_T and hence the molecular force parameters of neon. The experimetnal α_T values due to Maxwell's model-dependent and Slieker's model-independent column shape factors (CSF) together with the theoretical α_T values based on Chapman-Enskog gas kinetic theory[6] were also estimated. They are plotted against $\bar{T}$ in Fig. 9.2 for comparison. The experimental and theoretical F_s as well as the estimated experimental and theoretical α_T values are presented in Tables 9.1 and 9.2 respectively. The theoretical formulation of F_s is, however, derived in section 9.3 and is compared with the experimental F_s as seen in Fig. 9.3.

The plots of α_T against $\bar{T}$ obtained by the CCF method and of the collision integral C^*_{ij} against the reduced temperature $\bar{T}^*$ were simultaneously used to calculate the force parameters ε_{ii}/k or ε_{jj}/k of the isotopic components of neon. ε_{ii}/k or ε_{jj}/k are the depths of the potential well (see section 9.4). The molecular diameters σ_{ii} or σ_{jj} were then obtained from the coefficients of viscosity with the estimated force parameters (see Table 9.3). The excellent agreement of the force parameters with the literature values (Table 9.2) and the close agreement of α_T obtained by the CCF method with the theoretical ones as seen in Table 9.2 and Fig. 9.2 establish the fact that the derived relationship of F_s is reliable.

9.2. Formulations of the Experimental Thermal Diffusion Factor

Both ends being closed in an ideal TD column of length L, $\ln q_e$ is given by

$$\ln q_e = HL/(K_c + K_d) \qquad \text{..... (9.2)}$$

where q_e is defined by

$$q_e = (x_i / x_j)_{top} / (x_i / x_j)_{botom}$$

$(x_i / x_j)_{top}$ and $(x_i / x_j)_{bottom}$ represent the ratio of mole or mass fractions of lighter (i) and heavier (j) components of a binary gas mixture at the top and at the bottom of a TD column of geometrical length L. The column coefficients H, K_c and K_d are proportional to the second, fourth and zeroth powers of the pressure p in atmospheres respectively. On writing $H = H' p^2$, $K_c = K'_c p^4$ and $K_d = K'_d$ eq (9.2) can be put into the form

$$\ln q_e = \frac{(H' L / K'_c)p^2}{(K'_d / K'_c) + p^4}$$

or

$$p^2 / \ln q_e = b' / a' + (1/a')p^4 \qquad \text{..... (9.3)}$$

where $a' = (H'L / K'_c)$ and $b' = (K'_d / K'_c)$. The experimental parameters a' and b' of Table 9.1 govern the variation of the experimental $\ln q_e$ as a function of the pressure p in atmosphere at a given temperature. They were obtained from the measured values of H', K'_c and K'_d by Rutherford and Kaminsky[5]. The pressure dependences of $\ln q_e$ thus estimated are illustrated graphically in Fig. 9.1 by the fitted curves for four columns I, II, III and IV at various experimental temperatures. It is evident from eq (9.3) that , in each case seen in Fig. 9.1, as p increases $\ln q_e$ of the gas mixture increases and eventually reaches a maximum value of $\ln q_{max}$ given by

$$\ln q_{max} = \frac{a'}{2\sqrt{b'}} , \qquad \text{..... (9.4)}$$

at the optimum pressure P_{opt} given by $P_{opt} = (b')^{1/4}$ for which $(\delta/\delta p) \ln q_e = 0$. The experimental α_T or often the experimental F_s is obtained by using eqs. (9.1) and (9.4) in terms of F_s and $\ln q_{max}$ or α_T and $\ln q_{max}$.

Again, (9.2) on maximization becomes

$$\ln q_{max} = \frac{HL}{2(K_c K_d)^{1/2}} \qquad \text{..... (9.5)}$$

Table 9.1 The geometry of the columns with length L, cold wall radius r_c and hot wall radius r_h together with column constants G_1 and G_2, column calibration factor F_s, a', b' and $\ln q_{max}$.

Geometry of the column in m	Hot wall temp. T_h (K)	Cold wall temp. T_c (K)	Mean temp. $\overline{T}$ (K)	a' (atm^2)	b' (atm^4)	$\ln q_{max}$	Column constant $G_1(10^3)$	Column constant $G_2(10^5)$	Theoretical F_s from eq(9.14)	Experimental F_s
Column I										
$L = 3.05$										
$r_c = 1.6 \times 10^{-2}$								5.9120		
$r_h = 8.0 \times 10^{-4}$	1073	288	680.5	0.7367	0.0211	2.5358	4.3580		76.4942	91.8768
Column II										
$L = 3.05$	773	288	530.5	1.1982	0.0684	2.2907	3.2700	5.2986	76.4391	84.8407
$r_c = 1.27 \times 10^{-2}$										
$r_h = 8.0 \times 10^{-4}$	1073	288	680.5	2.0376	0.1282	2.8460	4.1831		97.7822	103.1159
Column III										
$L = 1.524$	473	288	380.5	1.0358	0.5498	0.6985	1.7285	4.4228	281091	27.0736
$r_c = 9.43 \times 10^{-3}$	773	288	530.5	2.3547	0.5902	1.5327	3.0576		49.7242	56.7667
$r_h = 8.0 \times 10^{-4}$	1088	288	688.0	4.7567	1.2955	2.0896	3.9524		64.2766	75.7101
Column IV										
$L = 1.524$	381	288	334.5	2.3265	4.6460	0.5397	0.7025	2.1957	18.2122	21.5880
$r_c = 9.43 \times 10^{-3}$										
$r_h = 3.2 \times 10^{-3}$	773	288	530.5	10.2385	5.2510	2.2340	2.9767		77.1747	82.7407

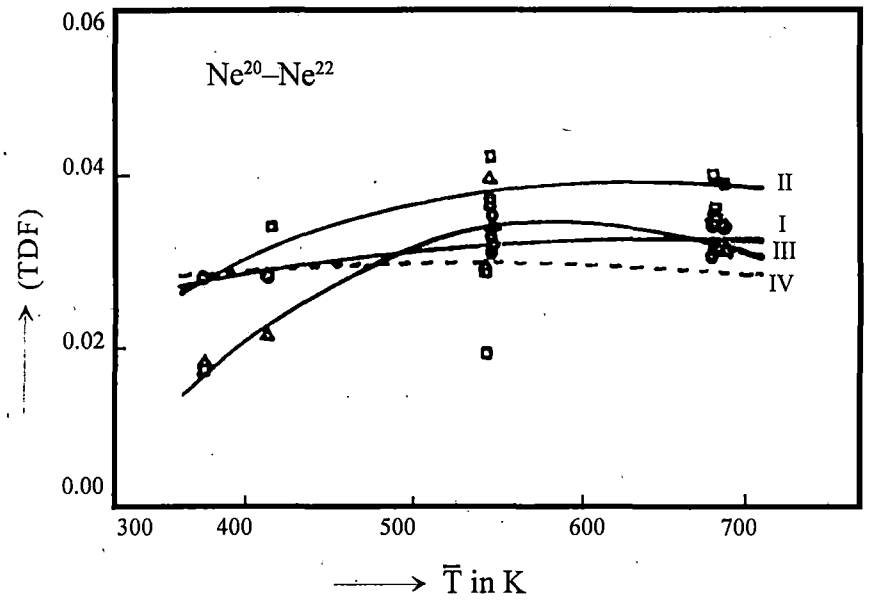

Fig. 9.2. A plot of TD factor α_T of Ne^{20}–Ne^{22} against $\bar{T}$ in kelvins : curve I, (O), by the CCF method; curve II, (Δ), due to the Slieker CSF; curve III, (□), due to the Maxwell CSF; and curve IV, (---), due to the elastic collision theory.

The column coefficients H, K_c and K_d based on Maxwell model dependent CSF h', k'_c and k'_d are[7]

$$H = \frac{2\pi}{6!}\left(\frac{\alpha_T \rho^2_{ij} g}{\eta_{ij}}\right)\frac{1}{2}(r_c + r_h)(r_c - r_h)^3\left(\frac{\Delta T}{\bar{T}}\right)^2 h'$$

$$K_c = \frac{2\pi}{9!}\left(\frac{\rho^3_{ij} g^2}{\eta^2_{ij} D_{ij}}\right)_1 \frac{1}{2}(r_c + r_h)(r_c - r_h)^7\left(\frac{\Delta T}{\bar{T}}\right)^2 k_c'$$

$$K_d = 2\pi(\rho_{ij} D_{ij})\frac{1}{2}(r_c + r_h)(r_c - r_h)k'_d.$$

The experimental α_T due to the Maxwell model dependent CSF is thus

$$\alpha_T \text{ (Maxwell model)} = 2.39\frac{r_c - r_h}{L}\frac{\bar{T}}{\Delta T}\frac{(k'_c k'_d)^{1/2}}{h'}\ln q_{max} \quad \ldots\ldots\ldots\ldots (9.6)$$

where $\Delta T = T_h - T_c$. Similarly the column coefficients due to the model-independent Slieker's[8] CSF $(SF)_1$, $\pi(1-a^2)$ and $(SF)_3$ are

$$H = (SF)_1 r_c^4 \frac{\alpha_T \rho^2_{ij} g}{\eta_{ij}}\left(\frac{\Delta T}{\bar{T}}\right)^2$$

$$K_d = \pi(1-a^2) r_c^2 p_{ij} D_{ij}$$

$$K_c = (SF)_3 r_c^8\left(\frac{\rho^3_{ij} g^2}{\eta^2_{ij} D_{ij}}\right)\left(\frac{\Delta T}{\bar{T}}\right)^2$$

where $a = r_h / r_c$. Using Slieker's CSF, α_T is given by

$$\alpha_T \text{ (Slieker)} = 2.0\frac{r_c}{L}\frac{\bar{T}}{\Delta T}\frac{[\pi(1-a^2)(SF)_3]^{1/2}}{(SF)_1}\ln q_{max}. \quad \ldots\ldots (9.7)$$

The experimental α_T values using the CSF were obtained from eqs. (9.6) and (9.7) together with those by CCF method from eq (9.1) in terms of measured $\ln q_{max}$ and F_s. All these α_T values are placed in Table 9.2 for comparison with the theoretical ones. They are also shown graphically in Fig 9.2 with respect to $\bar{T}$ for Ne^{20}-Ne^{22} gas mixtures. The corresponding CSF's based on Maxwell model dependent and Slieker model independent methods are entered in Table 9.3.

Table 9.2. Experimental and theoretical α_T at various experimental temperatures together with estimated force parameters ϵ_{ij}/k and molecular diameters σ_{ij}.

		Experimental α_T using				Estimated		Reported	
Column	Mean temp. $\overline{T}$ (K)	F_s of equation (9.14)	Slieker's shape factor	Maxwell's shape factor	Theoretical α_T using equation (9.15)	ϵ_{ij}/k (K)	σ_{ij} (10^{10} m)	ϵ_{ij}/k (K)	σ_{ij} (10^{10} m)
Column I	530.5	0.034	0.043	0.040	0.028				
	680.5	0.033	0.042	0.035	0.028				
Column II	530.5	0.030	0.037	0.033	0.028				
	680.5	0.029	0.036	0.029	0.028			47.0[a]	2.72[a]
						48.58	2.69		
								41.186[b]	3.07[b]
Column III	380.5	0.025	0.032	0.017	0.027				
	530.5	0.031	0.037	0.030	0.028				
	688.0	0.033	0.040	0.030	0.028				
Column IV	334.5	0.030	0.012	0.013	0.026				
	530.5	0.029	0.015	0.027	0.028				

a Clifford et al (1977)[13]
b Aziz (1976)[13]

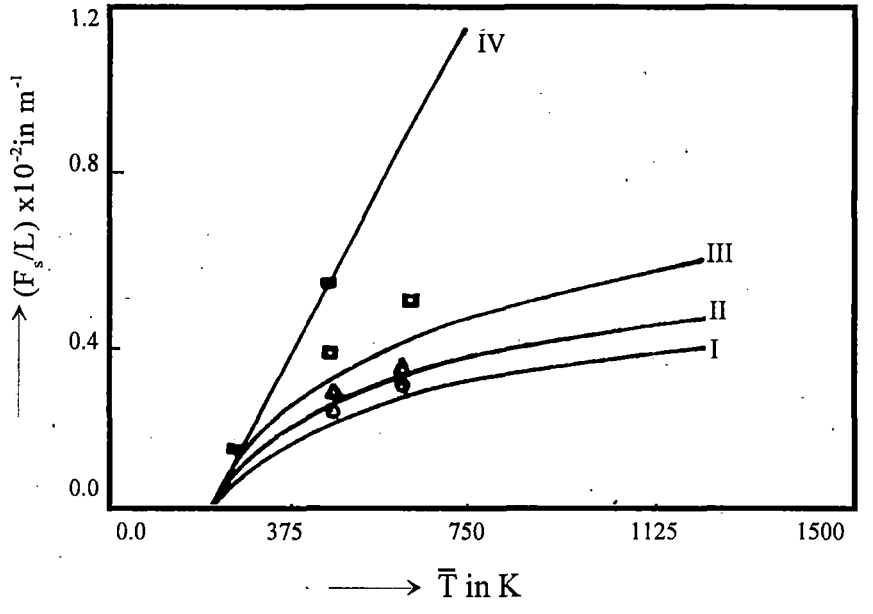

Fig. 9.3. A plot of the theoretical F_s (equation (9.14) with the experimental F_s on it against $\bar{T}$ in kelvins : curve I, for column I, (O) experimental points; curve II, for column II, (Δ), experimental points; curve III, for column III, (□), experimental points; and curve IV, for column IV, (■), experimental points.

9.3. The Theoretical Formation of the Column Calibration Factor

The column parameters in cylindrical coordinates derived from the most elementary theory of the thermal diffusion column by Cohen[9] are

$$H = 2\pi \int_{r_h}^{r_c} \alpha_T \frac{\delta}{\delta r}(\ln T)\, dr \left(\int_{r_h}^{r} \rho_{ij} \upsilon r\, dr\right),$$

$$K_c = 2\pi \int_{r_h}^{r_c} \frac{dr}{\rho_{ij} D_{ij} r} \left(\int_{r_h}^{r} \rho_{ij} \upsilon r\, dr\right)^2$$

and $$K_d = 2\pi \int_{r_h}^{r_c} \rho_{ij} D_{ij} r\, dr$$

which can, however, be approximated almost in the same manner as was done earlier by Slieker[8]. Here ρ_{ij} and D_{ij} are the density and diffusion coefficients of the gas mixture, r is the radial coordinate and T is the absolute temperature in kelvin.

Under the influence of the temperature gradient along the horizontal plane of the column, the convective velocity υ of the molecule in the vertical direction is obtained from the Navier-Stokes equation in cylindrical coordinates:

$$\frac{\delta^3 \upsilon}{\delta r^3} + \frac{1}{r}\frac{\delta^2 \upsilon}{\delta r^2} - \frac{1}{r^2}\frac{\delta \upsilon}{\delta r} = \frac{\rho_{ij} g}{\eta_{ij} \bar{T}} \frac{dT}{dr}.$$

If we consider the rectilinear flow of heat from the hot wire or wall of temperature T_h to the cold wall of temperature T_c of a TDC, the temperature T is given by

$$T = T_h - \frac{\Delta T}{r_c - r_h}(r - r_h)$$

Puting $r = e^x$ and solving the above equation, we get

$$v = C_1 + C_2 \ln r + C_3 r^2 - \frac{\rho_{ij} g}{\eta_{ij} \bar{T}} \frac{\Delta T}{(r_c - r_h)} \frac{r^3}{9}$$

Table 9.3. Maxwell model dependent and Slieker-model-independent column shape factors, coefficient of viscosity η_{ij} and thermal conductivity λ_{ij} of Ne^{20}–Ne^{22} gas mixture.

Column	Mean temp $\overline{T}$ (K)	Column shape factor: Maxwell h'	Maxwell k'_c	Maxwell k'_d	Slieker $(SF)_1(10^3)$	Slieker $(SF)_3(10^6)$	η_{ij} (10^5 kg m^{-1} s^{-1})	λ_{ij} (10^2 cal m^{-1} s^{-1} K^{-1})
	530.5	1.035	3.300	0.700			5.0333	1.7900
Column I					1.3639	1.9717		
	680.5	1.585	6.075	0.725			6.2543	2.2236
	530.5	1.060	3.100	0.715			5.0333	1.7900
Column II					1.3914	1.9140		
	680.5	1.600	5.525	0.740			6.2543	2.2236
	380.5	0.800	1.050	0.745			3.8123	1.3558
Column III	530.5	1.120	2.975	0.750	1.2838	1.6646	5.0333	1.7900
	688.0	1.590	4.975	0.770			6.3153	2.2459
	334.5	0.970	0.500	0.912			3.4378	1.2226
Column IV					239.23	4662.2		
	530.5	1.185	1.775	0.925			5.0333	1.7900

$$= Gr_c^2 (K_1 + K_2 \ln\phi + K_3\phi^2 + \phi^3) \quad \text{..... (9.8)}$$

where $K_1 = \frac{C_1}{Gr_c^2} + \frac{C_2}{Gr_c^2} \ln r_c$,

$$K_2 = \frac{C_2}{Gr_c^2}, \quad K_3 = C_3 / G$$

and $$G = \frac{\rho_{ij} g}{\eta_{ij} \bar{T}} \frac{\Delta T}{(a-1)} \frac{1}{9}.$$

C_1, C_2 and C_3 being the integration constant, $\phi = r/r_c$ is the new veriable and $a = r_h/r_c$. The boundary conditions are

i) $v = 0$ *at* $r=r_c$ for which $\phi = 1$

ii) $v = 0$ at $r=r_h$ for which $\phi = a$ and since there is no transport of components of the gas mixture at equilibrium in the vertical direction up and down the column, we have

(iii) $$r_c^2 \int_a^1 \rho v \phi d\phi = 0.$$

Here, K_1, K_2 and K_3 are dimensionless constants which are, however, given explicitly in terms of $a(= r_h/r_c)$ of a TDC by applying the boundary conditions mentioned above :

$$K_1 = \frac{5a^2(1-a)(1+2a^2 \ln a - a^2) + \ln a}{5(a^2-1)^2 + 5(1-2a^4)\ln a},$$

$$K_2 = \frac{5a^2(1-a)(1-2a^2) - (1-a^2)}{5(a^2-1)^2 + 5(1-2a^4)\ln a} \quad \text{and}$$

$$K_3 = -(K_1 + 1).$$

The column coefficients H, K_c and K_d are now derived as follows :

$$H = -2\pi r_c^2 \int_a^1 \alpha_T \frac{\delta}{\delta\phi}(\ln T)d\phi \int_a^{\phi} \rho_{ij} v\phi d\phi$$

$$= 2\pi\alpha_T \frac{\Delta T}{1\text{-}a} \rho_{ij} Gr_c^4$$

$$x \int_a^1 \frac{1}{T}\left[\left(\frac{K_1\phi^2}{2} + \frac{K_2\phi^2}{2}\left(\ln\phi - \frac{1}{2}\right) + \frac{K_3\phi^4}{4} + \frac{\phi^5}{5} + K_4\right]d\phi\right.$$

where $K_4 = -\frac{a^2}{2}\left[K_1 + K_2\left(\ln a - 1/2\right) + K_3 a^2/2 + 2a^3/5\right]$

Here, the temperature and composition dependences of n_{ij}, ρ_{ij}, D_{ij} and α_T are not taken into account[7-9] and the above equation for H becomes

$$H = 2\pi\alpha_T r_c^4 \frac{\rho_{ij}^2 g}{\eta_{ij}\bar{T}} \frac{\Delta T}{(a-1)9} G_1 \qquad \text{..... (9.9)}$$

where $G_1 = \frac{\Delta T}{\bar{T}(1\text{-}a)}\left(\frac{2K_1 - K_2}{12}(1 - a^3) - \frac{K_2}{18}(1\text{-}a^3)\right.$

$$\left. - \frac{K_2 a^3}{6}\ln a + \frac{K_3}{20} + K_4(1-a) + \frac{1}{30}\right)$$

$$- \left(\frac{\Delta T}{\bar{T}(1\text{-}a)}\right)^2 \left[\frac{2K_1 - K_2}{48} - \frac{K_2}{24}\left(7/12 + a^4 \ln a\right)\right.$$

$$\left. + \frac{K_3}{120} + \frac{K_4}{2}(1 - a^2) + 1/210\right]$$

$$+ \left(\frac{\Delta T}{T(1\text{-}a)}\right)^3 \left[\frac{2K_1 - K_2}{120} - \frac{47K_2}{3600} + \frac{K_3}{420} + \frac{K_4}{3}(1 - a^3) + 1/840\right]$$

..... (9.10)

rataining the term containing up to the third power of $\Delta T/[\bar{T}(1\text{-}a)]$ because the contributions of higher terms are negligibly small. Again, a^n is very small compared with unity for $n \geq 4$.

The coefficient K_c of a TDC is given by

$$K_c = 2\pi\int_a^{\phi} \frac{d\phi}{\rho_{ij} D_{ij} \phi}\left(\int_a^{\phi} \rho_{ij} v \phi d\phi\right)^2.$$

$$= \frac{2\pi\rho_{ij} G^2 r_c^8}{D_{ij}}\int_a^1 \frac{1}{\phi}\left[\frac{K_1\phi^2}{2} + \frac{K_2\phi^2}{2}\left(\ln\phi - \frac{1}{2}\right)\right.$$

$$\left. + \frac{K_3\phi^4}{4} + \frac{\phi^5}{5} + K_4\right]^2 d\phi$$

$$= \frac{2\pi\rho^3_{ij} g^2}{\eta^2_{ij} D_{ij}}\left(\frac{\Delta T}{\bar{T}}\right)\frac{r_c^8}{81(1\text{-}a)^2} G_2 \qquad \text{.....(9.11)}$$

Where $$G_2 = \frac{K_1^2}{16} + \frac{5K_2^2}{128} - K_4^2 \ln a + \frac{K_3^2}{128} - \frac{3K_1K_2}{32} + \frac{K_1K_3}{24}$$

$$+ \frac{K_1K_4}{2}(1-a^2) - \frac{K_2K_3}{36} + \frac{K_3K_4}{8} - \frac{K_2K_4}{4}(2+2a^2\ln a - a^2)$$

$$+ \frac{K_1}{35} - \frac{9K_2}{490} + \frac{K_3}{90} + \frac{2K_4}{25} + \frac{1}{250}. \qquad \text{..... (9.12)}$$

For column IV where a=0.34, the higher power of 'a' in G_2 i.e., $\frac{a^4}{32}[2K_1K_2 + K_2^2(\ln a - 1) - 4k_3k_4]$ is taken.

The coefficient K_d of a TDC is obtained as

$$K_d = 2\pi r_c^2 \int_a^1 \rho_{ij} D_{ij} \phi d\phi$$

$$= \pi r_c^2 \rho_{ij} D_{ij}(1-a^2). \qquad \text{..... (9.13)}$$

Thus the CCF per unit length , F_s/L, is finally obtained from eq. (9.5) with the help of eqs (9.9)-(9.13). It is given by

$$F_s / L = \frac{G_1}{r_c[2(1-a^2)\, G_2]^{1/2}}. \qquad \text{..... (9.14)}$$

The theoretical CCF per unit length of any TD column can thus be approximated in terms of G_1, G_2, a and r_c of the column. The values of formulated F_s are placed in Table 9.1 for columns I, II, III and IV. They are shown in Fig.9.3 together with the experimental F_s/L obtained from $\ln q_{max}$ and known α_T values of Ne^{20}-Ne^{22} gas mixtures. F_s / L of eq. (9.14) plays an important role in determining α_T of any binary gas mixture[1-4]. Because its model independency is well established[3], F_s/L can safely be used to concentrate impurities of any gas to any desired level in TDC experiments.

9.4. Force Parameters from the TD Factor

The theoretical α_T based on Chapman -Enskog gas kinetic theory[6] is given by

$$\alpha_T = g(6C_{ij}^* - 5) \qquad \text{..... (9.15)}$$

where $$g = \frac{1}{6\lambda_{ij}} \frac{S^{(i)} x_i - S^{(j)} x_j}{X_\lambda + Y_\lambda}$$

is a complicated function of the composition of the gas mixture and of the thermal conductivity λ_{ij} where as $(6C_{ij}^* - 5)$ strongly depends on the temperature. The λ_{ij}'s are, however, obtained from the η_{ij}'s by using the relation

$$\lambda_{ij} = (15R / 4M)\eta_{ij}$$

The experimental values of η_{ij} of the Ne^{20}-Ne^{22} gas mixture are taken from Yamamoto *et. al.*[10]. The estimated theoretical α_T values for Ne^{20}-Ne^{22} are shown by curve IV of Fig. 9.2 in which they are compared with α_T obtained by the existing method, curve II and curve III, due to the Maxwell and Slieker CSF's as well as with α_T values of curve I obtained by the CCF method.

Now, the slowly varying function of temperature g is given by[3,11]

$$g = A/(6C - 5)$$

A and C are two arbitrary constants. A is determined from α_T of the CCF method at two available temperatures $\bar{T}$ in kelvins and C from the reported data[12] of C_{ij}^* versus $\bar{T}^*$. Using the relation

$$(6C^*_{ij} - 5) = [(\alpha_T)_{expt}] / g \qquad (9.16)$$

the collision integral[12] C^*_{ij} fixes $\bar{T}^*$ where $\bar{T}^* = \bar{T} /(\varepsilon_{ij}/k)$ and hence ε_{ij}/k of the molecule is located. Because the variation of g with the temperature is very slow, the entire procedure with the initially estimated ε_{ij}/k is repeated to get the exact value of ε_{ij}/k. The molecular diameter σ_{ij} is then determined from the viscosity data[10] with the estimated ε_{ij}/k. It is worthy to mention that, in the case of isotopic components, the force parameters due to binary interactions ε_{ij}/k and σ_{ij} become ε_{ii}/k or ε_{jj}/k and σ_{ii} or σ_{jj} respectively.

9.5. Results and Discussion

The equations of $p^2 / \ln q_e$ against p^4 of Ne^{20}-Ne^{22} gas mixtures were, however, worked out in terms of the measured values of H', K'_c and K'_d[5] from the pressure dependences of $\ln q_e$ in four columns of different column geometries and at various experimental temperatures. They are for column I:

$p^2/\ln q_e$ = $0.0305 + 1.9290p^4$ at $\bar{T}$ = 530.5 K

$0.0286 + 1.3574p^4$ at $\bar{T}$ = 680.5 K

for column II :

$p^2/\ln q_e$ = $0.0571 + 0.8346p^4$ at $\bar{T}$ = 530.5 K

$0.0629 + 0.4908p^4$ at $\bar{T}$ = 680.5 K

for column III :

$0.5309 + 0.9654p^4$ at $\bar{T}$ = 380.5 K

$p^2/\ln q_e$ = $0.2506 + 0.4247p^4$ at $\bar{T}$ = 530.5 K

$0.2703 + 0.2102p^4$ at $\bar{T}$ = 688.0 K

for column IV :

$p^2/\ln q_e$ = $1.9970 + 0.4298p^4$ at $\bar{T}$ = 334.5 K

$0.5129 + 0.0977p^4$ at $\bar{T}$ = 530.5 K.

The variation of $\ln q_e$ with p in atmospheres is found to increase with increasing length L and r_h / r_c of the TD columns as shown in Fig. 9.1. p_{opt}, the optimum pressure at which $\ln q_e$ becomes maximum as observed in Fig. 9.1, also increases on going from column I to column IV for increasing r_h / r_c. The variation of

$p^2 / \ln q_e$ against p^4 is governed by a' and b' of eq (9.3). a' and b' were, however, obtained by applying a least square fitting technique to eq (9.3) with the experimental data[5] of H', K'_c and K'_d. They are placed in the fifth and sixth columns of Table 9.1. $\ln q_{max}$ in terms of a' and b' of eq (9.4) are also placed in the seventh column of Table 9.1.

An approximate formulation of theoretical F_s with the column geometry has been derived by considering the convective velocity of the molecules in a TD column from the Navier-Stokes equation in cylindrical coordinates. Rectilinear flow of heat from a hot wire or wall to a cold wall seems to be a better choice, unlike Slieker's derivation. Although the temperature and composition dependences of the transport parameters like p_{ij}, n_{ij}, D_{ij}, λ_{ij} and α_T were not taken into account, the derived relationship of F_s with the column geometry and the temperature is reliable, simple and straightforward. This is strictly valid in the case of a hot wire or cryogenic wall or even for a hot wall column.

The column constants G_1 and G_2 depending on the column geometry and wall temperatures were worked out for four columns and are placed in the eight and ninth columns of Table 9.1. F_s / L of each column at experimental temperatures were then determined using eq. (9.14) and are placed in the tenth column of Table 9.1. G_1 and G_2 of eqs (9.10) and (9.12) are dimensionless column constants, suggesting the fact that these parameters are indenpendent of the molecular model. G_1 depends on $\Delta T / \overline{T}$ and r_h/r_c of a TDC where as G_2 is expressed in terms of r_h/r_c alone. The physical meanings of G_1 and G_2 can be realized from eqs (9.9) and (9.11). G_1 is related to the column transport coefficient H which is involved in the process of thermal diffusion, whereas G_2 is related to K_c, occurring in a TD process. However, K_c and K_d are the longitudinal and back diffusion coefficients in a TDC. Nevertheless, G_1 and G_2 are of much importance for locating the exact values of F_s, α_T and p_{opt} at which $\ln q_e$ becomes maximum. The available α_T values of $Ne^{20} - Ne^{22}$ gas mixtures, which are 0.0250, 0.0258, 0.0270, 0.0276 and 0.0276 at 334.5 K, 380.5K, 530.5K, 680.5K and 688K respectively [5], help one to get experimental F_s at various values of $\overline{T}$ from estimated $\ln q_{max}$ of eq (9.4) of the TD columns. The experimental F_s when plotted against $\overline{T}$ in Fig. 9.3 are in close agreement with

theoretical F_s derived from eq (9.14) at various $\bar{T}$.

Using eq (9.1) the α_T values of Ne^{20}–Ne^{22} gas mixtures are estimated through theoretical F_s by the CCF method. These α_T values are presented in the third columns of Table 9.2 and plotted against $\bar{T}$ in Fig. 9.2. The experimental α_T values obtained by the CCF method from $\ln q_{max}$ and F_s are found to fall almost on the same curve I and increase slowly with $\bar{T}$.

The slight disagreement between the experimental and theoretical F_s seen in Fig 9.3. and Table 9.1 results in a slight difference between the theoretical α_T values and the experimental ones obtained by the CCF method. This may, perhaps, arise due to the effect of parasitic remixing in the thermal diffusion process.

The molecular force parameters of Ne^{20}-Ne^{22} were estimated from the slope and the intercept of the α_T against $1/\bar{T}$ equation. The α_T at 500.0 K and 600.0 K from curve 1 of Fig. 9.2 were found to obey an equation of the form $\alpha_T = 0.02913 - 1.12501(1/\bar{T})$. The molecular force parameters, ε_{ij}/k of Ne^{20}-Ne^{22} were thus determined as explained elsewhere [3,11]. The η_{ij} [10] of Ne^{20}–Ne^{22} were then used to obtain the molecular diameter σ_{ii} or σ_{jj}. The close agreement of the estimated force parameters, placed in Table 9.2 with the reported ones[13] establishes the reliability of α_T as obtained by CCF method.

The α_T due to Slieker's CSF, as seen in Table 9.3, are calculated from eq (9.7) and are placed in the fourth column of Table 9.2. These α_T values, although slightly higher in magnitude than the α_T values obtained by the CCF method, are plotted with $\bar{T}$ in Fig 9.2 on curve II. The α_T values from $\ln q_{max}$ of column IV are scattered (Fig. 9.2), but still maintain the same trend as that of the CCF method. The magnitudes of the Maxwell model dependent CSF are really very difficult to locate exactly. They were, however, obtained by interpolation and extrapolation from the data of Vasaru[7] and placed in Table 9.3. The probable temperature dependence of α_T using the Maxwell model dependent CSF was then obtained from eq (9.6) and shown in the fifth column of Table 9.2. They are plotted with $\bar{T}$ in Fig 9.2 on curve III, showing both the trend and the magnitude of α_T against $\bar{T}$. It fails to accord with α_T obtained by the other methods. The theoretical α_T values based on elastic collision among molecules were also calculated from eq (9.15) at 334.5 K, 380.5 K, 530.5K, 680.5K and

688.0K for Ne^{20}-Ne^{22} and placed in the sixth column of Table 9.2. These are plotted against $\overline{T}$ on curve IV of Fig. 9.2. Both the magnitudes and the trends of these α_T values are more or less the same as those of the α_T values obtaind from the CCF. It is also interesting to note that the theoretical α_T values of curve IV exhibit the same trend of increasing with temperature as do the α_T values obtained by the CCF method.

In fact, asymmetry in column geometry is an inherent property and as such it invites remixing. Thus in the TD column theory Furry and Jones[14] added a term K_p called the remixing coefficient, proportional to p^4 in the denominator of eq (9.2). Obviously in an ideal column K_p is supposed to be zero. Leyarovski et at[15] had shown that K_p never exceeds 20% of K_c. Thus, owing to remixing effects, the maximum error that creeps into F_s and hence into α_T is 9.54%. In spite of that the excellent agreement of the experimental α_T (curve I) and the theoretical α_T (curve IV) in Fig. 9.2 it is evident that eq (9.14) is reliable for F_s/L. Moreover, it indicates that K_p increases with $\overline{T}$ particularly after $\overline{T} = 2T_c$,; that is, remixing starts from $\overline{T} = 2T_c$ in a TD column.

The discussion above makes it clear that the theoretical formulation of the CCF, which is the central point of study in this paper, is a model independent parameter, as observed earlier[1,4, 8,16]. Furthermore, the α_T values obtained from the CCF with $\overline{T}$ of a binary gas mixture are convenient means of estimating the molecular force parameters like ε_{ij}/k and σ_{ij} of the molecules. The subject in this paper is thus related to the efficiency of the gas separation using thermal diffusion column to throw some light on the basic physical properties of a gas mixture through the CCF and α_T.

9.6. Conclusions

In fact, the theoretical background of the process of thermal diffusion simultaneously involved with longitudinal and back diffusion in a TDC is much too complicated. The presented mathematical formulation of eq (9.14), achieved so far, seems to be a significant improvement over the existing theories. Determination of F_s/L appears to be an important means of estimating the experimental α_T through $\ln q_{max}$, particularly when $\Delta T/\overline{T}$ is close to unity or

$\bar{T} = 2T_c$. When $\Delta T / \bar{T}$ is well above unity the experimental α_T obtained by the CCF method differs from the theoretical α_T. Again, experimental α_T values obtained by using Slieker model independent and Maxwell model dependent CSF's are low compared with theoretical α_T values in the lower temperature region. Asymmetry in column geometry through K_p may be a reason for such a deviation. The theoretical α_T derived from the elastic collision theory is not in good agrement with experimental α_T for the non-spherical molecules. Even in the case of spherical molecules, the agreement is no better. The model independent parameter F_s/L of eq (9.14) thus ought to be used to estimate α_T for the pair of molecules concerned through experimental lnq_{max} in the TDC. The procedure of determining α_T by the CCF method is, therefore, necessary in order to improve the theory for obtaining α_T for elastic or inelastic collisions among the molecules[17]. The simultaneous use of reliable α_T by the CCF method and C^*_{ij} against $1/\bar{T}$ and $1/\bar{T}^*$ respectively appears to be a unique method of locating the exact force parameters of the molecules too.

References

[1] S. Acharyya, I. L. Saha, A. K. Dutta and A.K. Chatterjee, J. Phys. Soc. Japan **56** (1987) 105.

[2] A.K Datta, G. Dasgupta and S. Acharyya, J. Phys. Soc. Japan **59** (1990) 3602.

[3] G. Dasgupta, N. Ghosh, N. Nandi and S. Acharyya, J. Phys. Soc. Japan, **66** (1997) 108.

[4] A. K. Datta and S. Acharyya, J. Phys. Soc. Japan, **62** (1993) 1527.

[5] W.M. Rutherford and K. J. Kaminsky, J. Chem. Phys. **47** (1967) 5427.

[6] S. Chapman and T.G. Cowling, The mathametical theory of non-uniform gases (1952) (London's Cambridge University Press).

[7] G. Vasaru, Tharmal Diffussion Column, Supplied by S. Raman (Bombay; BARC).

[8] C.J.G. Slieker, Ph.D thesis, (1964) Amsterdam University.

[9] K. Cohen, The theory of isotope separation, (1951) (New York ; McGraw Hill).

[10] I. Yamamoto, H Makino and A. Kanagawa, J. Nucl. Sci.Technol. **27**(1990) 156.

[11] G. Dasgupta, N. Ghosh, N. Nandi, A. K. Chatterjee and S. Acharyya, J. Phys. Soc. Japan, **65** (1996) 2506.

[12] M. Klein and F.J. Smith, Tables of Collision Integral for the (m,6) potential for the value of m, Arnold Engineering Development Centre, Air Force Systems Command, Arnold Air Force Station, Tennessee.

[13] G. C. Maitland, M. Rigby E.B. Smith and W.A. Wakeham, Intermolecular Forces; Their origin and determinaiton, (1981) (Oxford, Clarendon).

[14] W.H. Furry and R. C. Jones, Phys. Rev. **69** (1946) 459.

[15] E.I. Leyarovski, J.K. Georgiev and A.L. Zahariev, Int. J. Thermophys. **9** (1988) 391.

[16] J.A. Madariaga, J.L. Navarro, J.M. Saviron and J.L. Brun, J. Phys. A; Math. Gen. **16** (1983) 1947.

[17] T. K. Chattopadhya and S. Acharyya, J. Phys. B; At. Mol. Phys. **7** (1974) 2277.